Development and validation of a dynamic thermal model of a minibus using TRNSYS

Daniela C. Vásconez-Núñez,
José Gonzálvez-Maciá,
José Miguel Corberán and Jorge Payá*

Instituto Universitario de Investigación en Ingeniería Energética,
Universitat Politècnica de València,
Valencia, Spain
Email: davasnue@upvnet.upv.es
Email: jgonzalv@ter.upv.es
Email: corberan@iie.upv.es
Email: jorge.paya@iie.upv.es
*Corresponding author

Abstract: The current paper presents a dynamic thermal model of a vehicle including two thermal zones, one for the front region (driver) and one for the back (passengers). The model, developed in TRNSYS, is able to predict the cabin's thermal behaviour under variable ambient temperatures and solar radiation. A minibus was used to validate the model using experimental data for ambient temperature, solar radiation and the indoor temperature of a minibus parked both inside and outside a garage in Torino (Italy). The proposed model accurately reproduces the warm-up and cool-down of the cabin. In addition, the model has been used to calculate the cooling load of the cabin during a summer day, and to quantify the thermal loads under variable ambient conditions. In future work, the model will be used to predict the dynamic performance of the A/C system in an urban driving cycle and to optimise the compressor control strategy.

Keywords: automotive; dynamic thermal model; TRNSYS; experimental validation; vehicle air conditioning; two thermal zones.

Reference to this paper should be made as follows: Vásconez-Núñez, D.C., Gonzálvez-Maciá, J., Corberán, J.M. and Payá, J. (2018) 'Development and validation of a dynamic thermal model of a minibus using TRNSYS', *Int. J. Vehicle Design*, Vol. 77, Nos. 1/2, pp.87–107.

Biographical notes: Daniela C. Vásconez-Núñez received her MSc at Universitat Politècnica de València (UPV) and is PhD student in the Instituto Universitario de Investigación en Ingeniería Energética at the same university. Her research interests include the air conditioning systems for the automotive industry.

José Gonzálvez-Maciá is tenure Professor at the Department of Applied Thermodynamics in UPV. He is Mechanical Engineer since 1997 and is an expert in refrigeration and heat pump systems, with more than 26 publications in research journals.

José Miguel Corberán is tenure Full Professor at the Department of Applied Thermodynamics in UPV. He is Head of the Instituto Universitario de Investigación en Ingeniería Energética and committee member in EUROTHERM (refrigeration) and in the Heat Pump Experts of the Spanish Ministry for Industry. He has published more than 70 papers in research journals.

Jorge Payá is a Mechanical Engineer since 2006 through UPV and the Ecole Centrale Paris. He is an Assistant Professor at the Applied Thermodynamics Department in UPV. He is corresponding author of more than 10 papers in first quartile research journals in the field of refrigeration and thermal energy storage.

1 Introduction

Nowadays, all types of vehicles such as buses, vans, cars and trucks are equipped with an air conditioning (A/C) system. The main function of the A/C system is to regulate the temperature and maintain a comfortable range of humidity of the air inside the cabin. In order to do so, the A/C system recirculates and refreshes the stale air from the cabin. However, using the A/C system increases the power consumption of the vehicle and also produces greenhouse gasses. The International Organization of Motor Vehicle Manufacturers (n.d.) estimates that around 16% of global man-made CO_2 emissions derive from road transport (cars, trucks, and buses), which represents around 13% of the total greenhouse gas emissions.

Consequently, the energy consumption of a vehicle depends on the design and size of the A/C system. The A/C system is affected directly by the thermal loads which heat the vehicle cabin. The thermal loads are mainly influenced by solar radiation, convective heat transfer with the external air, and internal gains such as the occupancy, auxiliary equipment, and ventilation.

Some studies have been published about thermal models of vehicle cabins in order to study their thermal behaviour and comfort levels. These studies can be divided into two groups, whether they are based on lumped-parameter models or on computational fluid dynamics (CFD) analyses.

Mezrhab and Bouzidi (2006) studied the effects of solar radiation, glazing type, car colour and radiative properties of the cabin materials. A nodal method and a finite difference method were employed. The compartment was subdivided into several solid (i.e., materials) and fluid (i.e., volumes of air) nodes. Conceição et al. (1999) developed a model based on the space-integral energy balance equations for the air inside the cabin and for the surrounding surfaces; it was based on the model from Shimizu et al. (1984), which included a nocturnal heat balance and the division of the vehicle ceiling and side panels in different slices. The cited model also incorporated an internal calculation of the convective heat transfer coefficients. The model validation was performed using a railway car in summer conditions. Marcos et al. (2014) developed a dynamic thermal model in Matlab for a vehicle cabin, based on the theoretical heat transfer and including the thermal inertia. The latter model was validated under three conditions, some of which were with solar radiation. Akyol and Kilic (2010) developed, in Matlab-Simulink, a dynamic model of an automobile compartment, to study the impact of solar irradiation on

the cabin surfaces and on the thermal interactions between the driver and the passenger interior.

Torregrosa-Jaime et al. (2015) developed a transient thermal model of the cabin of a minibus in Matlab including a two-node model for the internal air. The model was validated using experimental data under different ambient conditions, including solar radiation. Lee et al. (2015) developed a model of a passenger car's cabin, considering solar radiation, engine heat through the firewall, and engine heat to the air ducts. Several operating conditions were considered to obtain transient temperature profiles of the internal mass and cabin air for both idle and driving states. The model was validated with experimental data, and then applied to evaluate the mobile A/C system's design. Levinson et al. (2011) developed a thermal model to study the reduction of the soak temperature and A/C capacity using solar reflective car shells in either a black or silver colour. They determined that the A/C capacity required to cool the cabin air in the silver car to 25°C within 30 min is 13% less than that required for the black car.

Dullinger et al. (2015) presented a simulation tool to calculate the annual energy consumption of the heating, ventilating, and air conditioning (HVAC) system of a light rail vehicle. This included a dynamic thermal vehicle model and a modular structured HVAC model. The simulation tool was validated using real data in a tram. Pokorny et al. (2014) developed a mathematical model for the transient prediction of the indoor climate and the heat loads in a car cabin. The model is based on heat balance equations between the environment in the cabin and the outdoors, and considers different types of materials and thickness for each surface of the cabin. Roy et al. (2003) developed a model based on the concept of software assembly in which the surfaces of the vehicle are represented by plane elements which receive the variable solar flux.

Sevilgen and Kilic (2010) used a three-dimensional CFD model of a vehicle cabin to determine the airflow and heat transfer characteristics inside the vehicle cabin during a heating period as well as the heat transfer between human body surfaces and cabin environment. Fayazbakhsh and Bahrami (2013) developed a model of a vehicle cabin in C++ language to simulate real-time control of the A/C system, including a compressor, heat exchanger fans, passenger's seat temperatures and window glazing. The simulation results showed that some loads such as the engine, exhaust, and reflected radiation are often negligible, while others such as the ambient or ventilation load have a bigger impact on the cabin temperature.

Among the literature previously mentioned, most of the published work refers to lumped parameter models. CFD models (Fayazbakhsh and Bahrami, 2013; Roy et al., 2003; Sevilgen and Kilic, 2010) provide detailed spatial temperature distributions and air-flow fields inside the cabin. The sizing and operation of the A/C system does not necessarily require such detail, and a mean temperature distribution is sufficient to reach a good compromise between accuracy and computational cost. Previous CFD models have been employed to determine the heat transfer between human body surfaces and the cabin environment, but the A/C system has not been modelled. The published lumped parameter models have been adopted as the model-based control of the A/C system (Dullinger et al., 2015; Lee et al., 2015), and other authors have focused on the validation of internal temperatures with dynamic experimental tests (Akyol and Kilic, 2010; Conceição et al., 1999; Levinson et al., 2011; Marcos et al., 2014; Mezrhab and Bouzidi, 2006; Torregrosa-Jaime et al., 2015).

Regarding the studies cited previously, Lee et al. (2015) performed a test while driving, under climatic chamber conditions with a constant vehicle speed. Marcos et al. (2014) and Pokorny et al. (2014) presented the evolution of the internal temperature in a driving test, but the test conditions are not described in detail. Studies made with a moving vehicle are complicated to perform due to the difficulty of handling aspects such as variable wind speed, shadows of external buildings or elements, heat delivered by the engine, variable passenger occupancy, etc.

To our knowledge, there are no published thermal models of a vehicle developed in TRNSYS. Thermal models of vehicles are a simplification of the real problem, which is very complex to model since

- the geometry of the vehicle is not straightforward
- the exact materials of the different layers are generally unknown as well as their detailed thermo-physical properties
- the vehicle is not air-tight at all and infiltrations play an important role.

In this context, TRNSYS can be an useful tool to solve some of the modelling issues mentioned above.

The current paper presents a dynamic thermal model of the vehicle cabin developed in TRNSYS. A significant contribution of this work is that it presents a step-by-step procedure to develop and validate a thermal model, starting with tests under more controlled conditions (inside a garage) up to tests with dynamic ambient conditions (solar radiation, wind speed, etc.). Once developed, the model can be used as a tool to design the A/C system in real operating conditions or to optimise the operation of the compressor. This paper begins with the description of the experimental tests (Section 2). The model is described in Section 3, including the vehicle layout, the governing equations, and the constructive materials. Section 4 presents the model validation and the overall analysis of the cooling demand to maintain comfort conditions inside the cabin.

2 Experimental tests and measurement conditions

The tested vehicle is an Iveco Daily Electric minibus. Given the complexity of the problem, specific experimental tests have been conceived to validate the vehicle model. The first step is to validate the thermal model with tests which do not have any solar radiation (test 1 in Table 1); this was realised with tests inside a garage under controlled conditions, and helped to validate the model of the different wall layers.

The subsequent tests included variable outdoor conditions including solar radiation (tests 2 and 3) and enabled the validation of the full model taking into account the different solar radiation on each side of the vehicle. Table 1 details the conditions of the tests along with the instrumentation placed in the minibus (Figure 1).

2.1 Experimental test 1 (without solar radiation)

Experimental test 1 consists of warming up the internal air of the minibus for an amount of time, then letting the minibus air cool down and observing the thermal behaviour of the cabin during warm-up and cool-down. This test was carried out with the minibus parked inside a garage. The purpose of experimental test 1 is to validate the model

excluding the impact of solar radiation and to define the convective heat transfer coefficients between the vehicle surfaces and the indoor/outdoor air.

Table 1 Summary of the tests and measurement equipment

Test	*Test 1*	*Test 2*	*Test 3*
Conditions	Inside a garage	Parked outdoors with front facing west.	
Objectives	Validate the model without solar radiation	Validate the model under dynamic outdoor conditions (solar radiation and ambient temperature).	
Dates	03/07/2012	20/07/2012 To 23/07/2012	07/07/2012 To 09/07/2012
Duration (h)	6	82	54
Instruments	*T*-Type thermocouples with an uncertainty of ± 0.5 K	*T*-Type thermocouples with an uncertainty of ± 0.5 K. Pyranometer Lp pyra 02 delta ohm (uncertainty 1.5% at T_{amb} 23°C and 50% RH).	
Measured variables	Air temperatures inside and outside the vehicle	Air temperatures inside and outside the vehicle. Global solar irradiance on a horizontal surface.	

Figure 1 Location of the thermocouples: (a) test 1 and (b) tests 2 and 3 (see online version for colours)

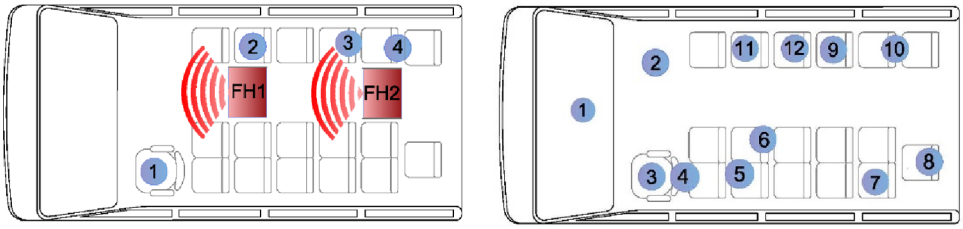

(a) (b)

To heat the vehicle cabin, two electrical fan-heaters (FH) of 2 kW were positioned along the corridor of the minibus. At the beginning of the test, the fan-heaters were turned on to heat up the minibus cabin. After 160 min, the fan-heaters were turned off, and the cabin cooled down due to natural convection. The entire experiment lasted 360 min, and the temperature measurements were registered every 30 s.

The temperature of the air inside the cabin was measured with four thermocouples placed in four locations at passenger head level. Figure 1(a) shows the location of the electrical fan heaters (FH1 and FH2) and the thermocouples.

2.2 Experimental tests 2 and 3 (with solar radiation)

Experimental tests 2 and 3 consisted of parking the minibus outside the garage and registering the internal air temperature of the minibus during 82 h (test 2) and 54 h (test 3). These tests were carried out with the minibus parked under the sun with the front facing west. The purpose of experimental tests 2 and 3 is to validate the model and to analyse the evolution of the internal air temperature under the incidence of solar radiation and ambient temperature.

The minibus was equipped with 12 thermocouples placed inside the cabin, and two thermocouples were placed outside the cabin to measure the ambient temperature. Figure 1(b) shows the location of the internal thermocouples. The global solar irradiance on the horizontal surface was measured by a pyranometer located on the roof of the minibus.

3 Model description

The thermal model of the minibus was developed using the transient system simulation software TRNSYS, which is a flexible software program used to simulate the performance of transient energy systems. In order to build the system model, TRNSYS uses components or types based on mathematical models written in ANSII standard Fortran (TRNSYS v. 16.1, 2007). The components or types of TRNSYS require several time-dependent inputs and outputs, which are interconnected between the different components as represented in Figure 2 for tests 2 and 3. The standard inputs and outputs used in the simulation are shown in this figure.

Figure 2 TRNSYS overall project to simulate the minibus under dynamic ambient conditions (tests 2 and 3) (see online version for colours)

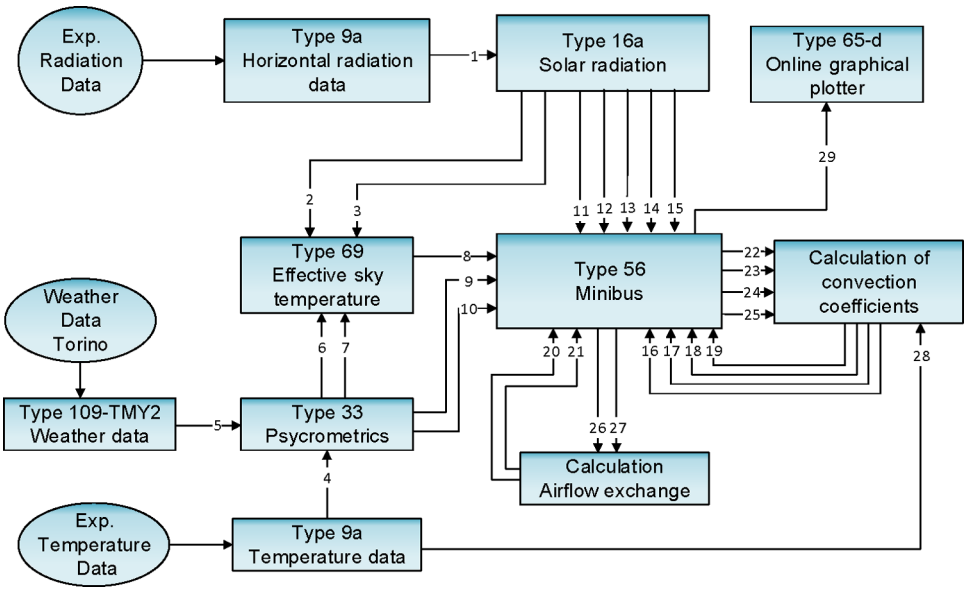

The main component of the model is Type 56, which simulates the thermal behaviour of a closed volume. A 0-D transient model is used to represent the thermal capacities of the air volume in a thermal zone. The zone air node exchanges heat by convection with the surrounding walls and windows, by infiltration, and by internal gains (people, equipment). The air balance equation gives the first order derivative of the air temperature. Wall heat transfer is calculated using a 1-D transient model that is solved using heat transfer functions. Internal wall and window temperatures in each time step are

calculated using a heat balance including convection and radiation. More details of the solver used can be consulted in TRNSYS 16 Documentation (2007).

Type 56 was adapted to simulate the thermal behaviour of the minibus considering two thermal zones (see the minibus scheme in Figure 3), zone 1 for the driver (front region) and zone 2 for the passengers (back region). In this type, specific parameters were defined for each zone in the TRNSYS type manager (walls, windows, layers, gains, infiltrations and others). As can be seen in Figure 2, Type 56 uses the following inputs:

- the incident solar radiation on each surface of minibus (11, 12, 13, 14 and 15) from Type 16a
- the effective sky temperature (8) from Type 69
- the dry bulb temperature and relative humidity percentage of the external ambient air (9, 10) from Type 33
- the internal and external convective heat transfer coefficients of the minibus surfaces (16, 17, 18 and 19)
- the air circulation between the zones (20 and 21).

The incident solar radiation on each surface of the minibus body is provided by Type 16a. This type estimates the total, beam and sky-diffuse radiation considering the latitude, slope, and azimuth of the surfaces. Type 16a uses the experimental data of solar irradiance on a horizontal surface (1), which is read by Type 9a from an external file.

Figure 3 Thermal zones of the vehicle model

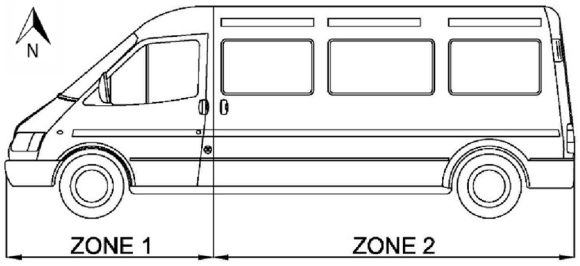

The effective sky temperature (8) is calculated by Type 69 as a function of the beam radiation (2), the diffuse radiation (3), the dry bulb temperature (6) and the dew point temperature (7) of the external air. The dry bulb and dew point temperature of the external air are obtained from Type 33.

Type 33 calculates the psychometric variables of the external air using experimental external air temperature and relative humidity data. The external air temperature is read by another Type 9a from an external file. The relative humidity is obtained from Type 109, which reads the weather data of Torino (Italy) from a TRNSYS database.

Type 65-d 'online graphical plotter' provides the internal air temperature for each zone at any time step of the simulation (29).

The external convective heat transfer coefficients were estimated using a calculator tool (Figure 2), which requires input of the experimental air temperature data (from Type 9a) and the external surface temperatures (from Type 56). Given the minimal air

speeds reached in the parking spot of the minibus, only natural convection has been considered for all external and internal surfaces.

The convective heat transfer coefficients depend on the temperature difference between the surface and the external air, and are therefore time-dependent. The external convective heat transfer coefficients are calculated with equation (1) (Incropera et al., 2007). This equation correlates natural convection using a Rayleigh number and an average Nusselt number which are defined based on the characteristic length of the surface in the specific direction (vertical and horizontal) and the flow regime (laminar or turbulent).

$$\bar{h} = \frac{\overline{\mathrm{Nu}}_L . k}{L} \tag{1}$$

The Nusselt number depends on the Rayleigh number, which is calculated for the top and bottom surfaces of cold and hot plates respectively, according to thermo-physical properties of the air using equation (2) (Incropera et al., 2007). Note that g is replaced by (g*Cosθ).

$$\mathrm{Ra}_L = \frac{g L^3 \beta \left(T_{\mathrm{surf}} - T_{\mathrm{amb}}\right)}{\nu \alpha_{\mathrm{Ra}_L}} \tag{2}$$

Table 2 summarises the correlations used for calculating the average Nusselt number for the vertical and horizontal surfaces of the minibus.

Table 2 Average Nusselt number correlations for external natural convection within the minibus surfaces

Vertical surfaces (*laminar and turbulent flow*)	
$\overline{\mathrm{Nu}}_L = \left\{ 0.825 + \frac{0.387 \mathrm{Ra}_L^{1/6}}{\left[1 + \left(0.492/\mathrm{Pr}\right)^{9/16}\right]^{8/27}} \right\}^2$ entire range of Ra_L	
Horizontal surfaces	
Upper surface of hot plate	*Lower surface of hot plate*
$\overline{\mathrm{Nu}}_L = 0.15 \mathrm{Ra}_L^{1/3}$	$\overline{\mathrm{Nu}}_L = 0.52 \mathrm{Ra}_L^{1/5}$
$10^7 \le \mathrm{Ra}_L \le 10^{11}$, all Pr	$10^4 \le \mathrm{Ra}_L \le 10^9$, $\mathrm{Pr} \ge 0.7$

The model obtains the properties of the air at each instant of time, according to the temperature of the external surfaces and the ambient air temperature. All air properties are evaluated at the film temperature (T_f) of equation (3).

$$T_f = \frac{T_{\mathrm{surf}} + T_{\mathrm{amb}}}{2} \tag{3}$$

For the natural convection inside the cabin, the TRNSYS option ‘internal calculation’ has been adopted. Between the two thermal zones, there is no physical barrier, therefore, the air circulates freely. In the literature, the airflow exchange has been analytically

obtained for other arrangements, but not for this particular configuration without a physical barrier. The airflow is clearly dependent on the air temperature, relative humidity, and density of the internal air. As a first approach, the airflow exchange between the driver and passengers is calculated using the air exchange equation (4) developed by Gosney and Olama (1975) for fully established flow. This equation is generally used to estimate the flow of cold and warm air masses for typical open freezer doors (ASHRAE, 2014).

$$\text{Air exchange} = 0.221A\left(1-\frac{\rho_1}{\rho_2}\right)^{0.5}(gH)^{0.5}F_m \tag{4}$$

In equation (4), A represents the area of air exchange between two zones, ρ_1 and ρ_2 are the density of infiltration air of the warmer and cooler zone respectively, g is a gravitational constant and F_m is the density factor calculated using equation (5).

$$F_m = \left(\frac{2}{1+\left(\frac{\rho_1}{\rho_2}\right)^{1/3}}\right)^{\frac{1}{5}} \tag{5}$$

Figure 4 shows the temperature difference between the two thermal zones of the vehicle cabin with and without air exchange. If no air exchange is assumed, the temperature difference between the two zones is up to 11 K. The model minimises the mean square error with respect to the measurements using equation (4) with a multiplying factor of 4, which is logical since the underlying physics are not identical. Figure 5 shows the airflow exchanged between two zones of the test 2.

Figure 4 Temperature difference between driver and passenger zones (test 2) (see online version for colours)

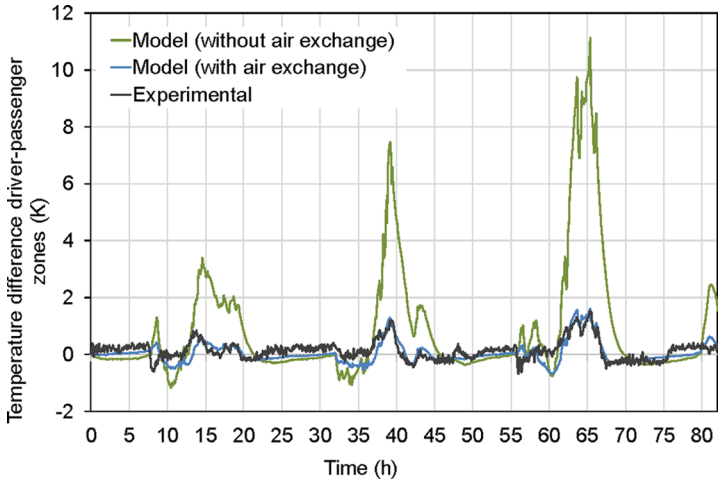

Figure 5 Airflow exchanged between driver and passenger zones (test 2) (see online version for colours)

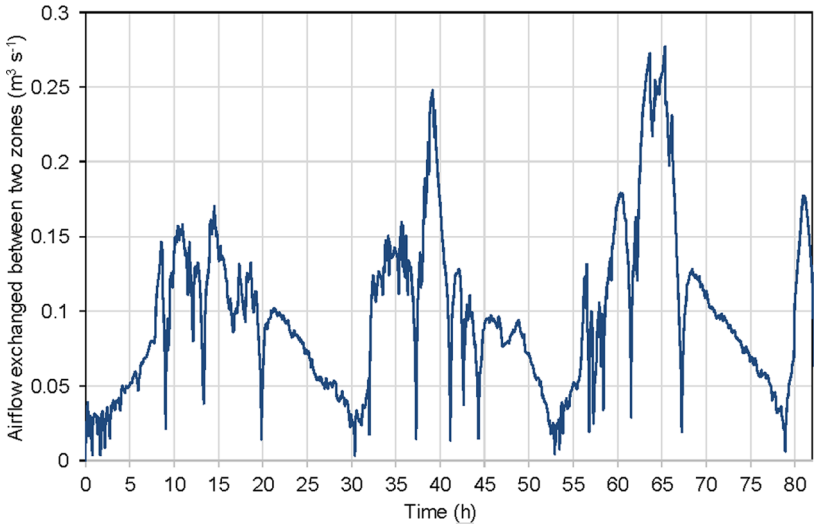

Owing to the small temperature difference between the two thermal zones (1.5 K), the minibus could also be modelled using a single thermal zone. However, a two-zone model was chosen because the incidence of solar radiation is different in each zone of the minibus cabin, and thus the thermal load is not the same in both. Local climate control could be hereby introduced in future work as a strategy to reduce the A/C energy consumption.

Figure 6 shows the types used in the model for test 1 (garage conditions), where the main difference is the lack of solar radiation and the use of fan heaters to heat up the cabin. The following types were not used in the model: Type 16a, Type 109-TMY2, Type 69 and Type 33.

Figure 6 TRNSYS overall project to simulate the minibus in garage conditions (test 1) (see online version for colours)

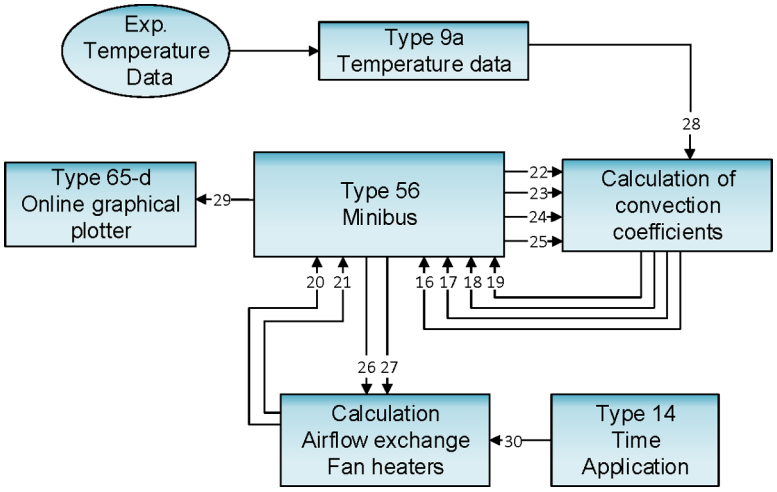

Type 9a reads the experimental air temperature data obtained inside the garage. These temperatures are read by Type 56. The fan heater loads (2 kW) are introduced in Type 56 through a calculator tool and the operation schedule of the fan heaters are simulated with Type 14. The convective coefficients are estimated with another calculator tool, which uses equations (2) and (3).

TRNSYS allows selection between three numerical algorithms to solve differential equations (modified-Euler method, non-self-starting Heun's method, fourth-order Adams method). In the present study, the Euler method has been chosen as it is the most consistent with the analytical method for solving the underlying differential equations of the model. The time step used in the simulations is 2 min, in accordance with the monitoring time step for the temperatures and solar irradiance. The physical duration of each simulation is 3, 4.5 and 6 s for tests 1, 2, and 3, respectively (corresponding durations of 6, 81 and 52 h). The simulation duration is based on a computer with the following specifications: Intel(R) Core(TM) i5-4430 CPU @ 3.00GHz RAM installed 4.00 GB, 64 bits.

3.1 Minibus dimensions and material composition of surfaces

The minibus surfaces are composed of several material layers of different thicknesses, areas, and thermo-physical properties. The dimensions of the minibus were obtained from manufacturer data, and are listed in Table 3.

The materials were selected based on the technical specifications of the minibus manufacturer data and on published literature (Conceição et al., 1999; Pokorny et al., 2014). Table 4 summarises the material composition of the minibus surfaces and their main properties. The values of the material properties were obtained from the TRNSYS library.

Table 3 Dimensions of the minibus

Surface	*Zone 1* [m^2]	*Zone 2* [m^2]
Roof	3.54	8.74
Floor	3.54	8.74
Right wall	2.39	8.71
Left wall	2.39	8.71
Front wall	2	–
Rear wall	–	3.65
Right window	0.82	2.45
Left window	0.54	2.45
Front window	–	0.747
Rear window	1.21	–

Infiltrations can vary depending on the vehicle size and the ambient air speed. The infiltrations in the model have been established in agreement with published literature (Knibbs et al., 2009; Ott et al., 2008) which considered the infiltrations in parked vehicles with the windows closed and the ventilation system off.

Table 5 presents the radiation heat transfer parameters for the minibus. They are obtained from the literature and are coherent with the existing models (Torregrosa-Jaime et al., 2015). The internal masses of the minibus are the driver's seat, front panel (zone 1), and 17 passenger seats (zone 2). The materials and dimensions of the internal masses were obtained from the minibus manufacturer.

Table 4 Material composition of the minibus surfaces

Layer	*Material*	*Thickness* [m]	*Conductivity* [kJ h^{-1} m^{-1} K^{-1}]	*Heat capacity* [kJ kg^{-1} K^{-1}]	*Density* [kg m^{-3}]
Roof	Polyvinyl chloride	0.004	0.92	1.17	1450
	Polyurethane	0.015	0.08	1.47	35
	Steel	0.002	160	0.51	7800
Floor	Polyvinyl chloride	0.006	0.92	1.17	1450
	Polyurethane	0.020	0.08	1.47	35
	Wood	0.015	0.468	1.88	650
	Steel	0.002	160	0.51	7800
Left, right, front and rear	Polyvinyl chloride	0.009	0.92	1.17	1450
	Polyurethane	0.017	0.468	1.88	650
	Steel	0.002	160	0.51	7800

Table 5 Radiative heat transfer parameters

Absorptivity of cabin walls	0.19
Absorptivity of internal masses	1
Emissivity of white paint	0.95
Emissivity of internal masses	1
Transmissivity of regular glass	0.8
Transmissivity of tinted glass	0.6

4 Results and discussion

4.1 Experimental test 1

Figure 7 depicts the experimental and simulated data for the air temperature inside the cabin during test 1. The temperatures shown are only for zone 2, as they are comparable to those for zone 1. In fact, with no physical barrier and with similar thermal conditions in each zone (e.g., no solar radiation) the maximum temperature difference reached between the two zones is only 0.7 K.

In the first 15 min, the air temperature increased rapidly to 35°C, then the air temperature rose almost linearly up to 50°C. Once the fan-heaters were turned off (after 2.7 h), the air temperature dropped quickly for the first 15 min. After that, the cooling rate was lower due to the impact of the thermal inertia of the internal masses. As can be seen in Figure 7, the developed model accurately reproduces the dynamic warm-up and cool-down of the cabin.

Figure 7 Experimental and simulation results of the air temperature inside the cabin (test 1, zone 2) (see online version for colours)

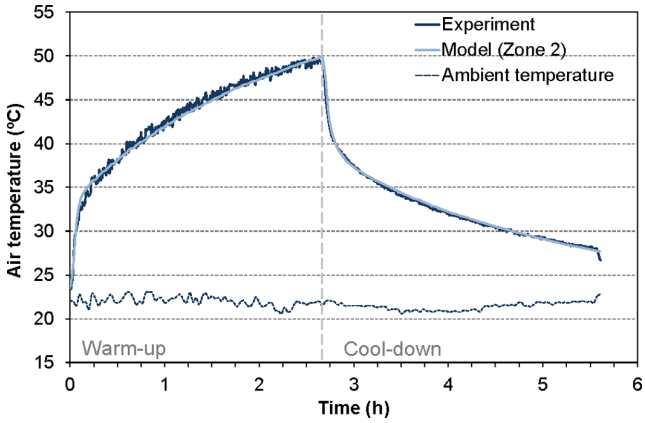

Figure 8 Ambient temperature and global horizontal irradiance: (a) test 2 and (b) test 3 (see online version for colours)

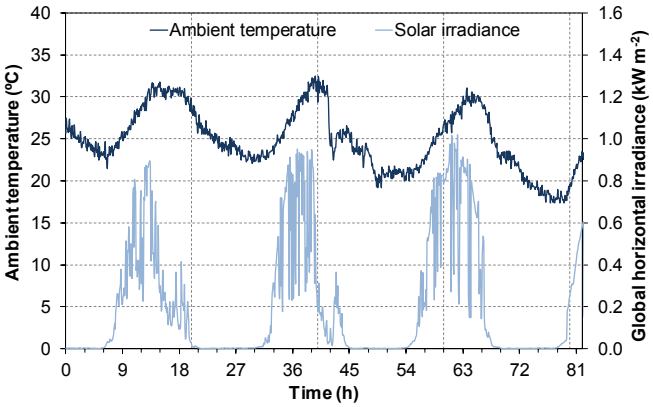

(a)

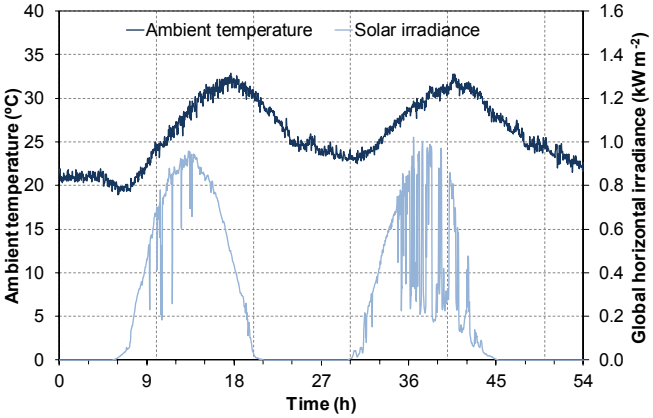

(b)

4.2 Experimental tests 2 and 3

Figures 8(a) and (b) illustrate the ambient temperature and the global horizontal irradiance measured during tests 2 and 3, respectively. The radiation curves are not uniform; they present sudden drops when the environment is cloudy (values down to 0.2 kW m^{-2} which correspond to diffuse radiation). The temperature curves present fluctuations which correspond to the solar irradiance, but the variations are small.

Figures 9 and 10 show the experimental and simulated results of the air temperature inside the cabin during tests 2 and 3, respectively. As in test 1, the air temperature values obtained for zone 1 are very similar to those for zone 2. According to the experimental data, the maximum temperature difference between the zones is 1.5 K for test 2 and 2.5 K for test 3. These temperature differences are higher than those observed in test 1. This is due to the solar radiation, which does not influence each thermal zone of the vehicle in the same way.

Figure 9 Experimental and simulation results of the air temperature inside the cabin (test 2, zone 2) (see online version for colours)

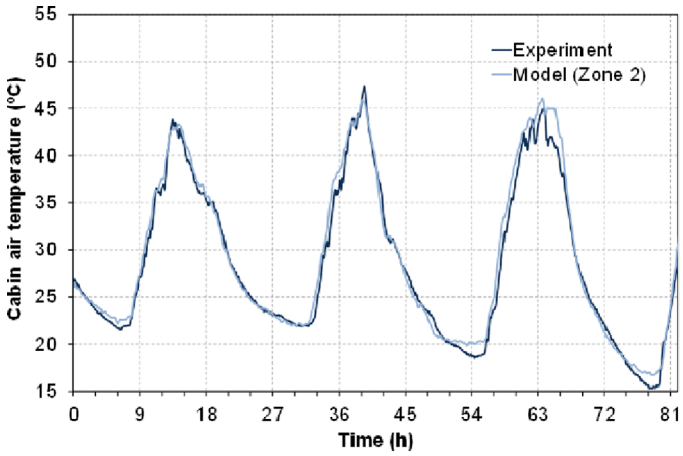

Figure 10 Experimental and simulation results of the cabin air temperature (test 3, zone 1) (see online version for colours)

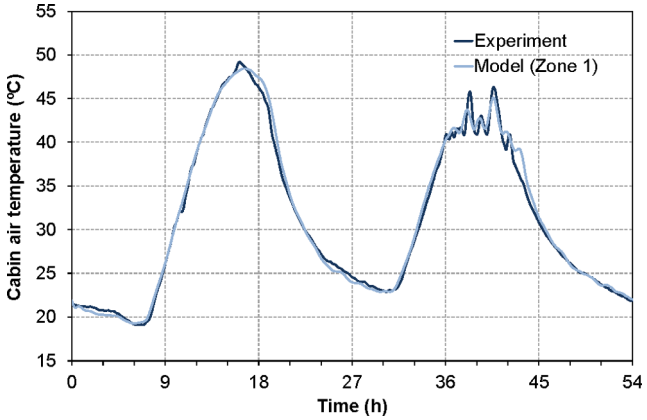

As can be observed in Figures 9 and 10, the solar irradiance directly affects the air temperatures inside the cabin, inducing high temperatures at mid-day. The model accurately predicts the experimental trends.

Figure 11 Experimental and simulation results of the internal mass temperature: (a) test 2 and (b) test 3 (see online version for colours)

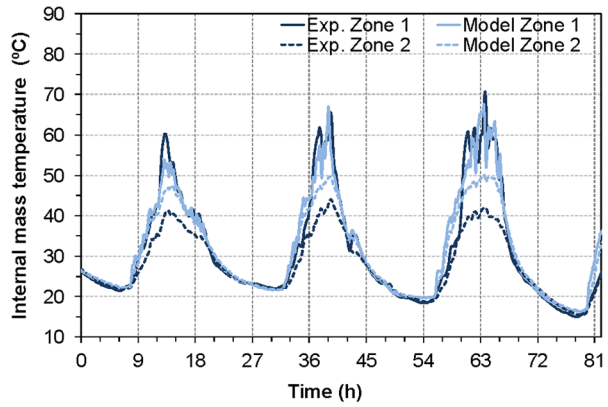

(a)

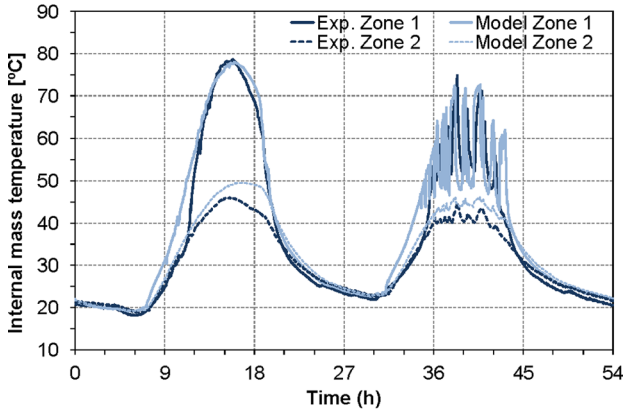

(b)

Figures 11(a) and (b) show the internal masses temperature for tests 2 and 3, respectively. The internal masses in zone 1 reach higher temperatures than those in zone 2, for the following reasons:

- in the afternoon, solar radiation directly affects zone 1 because the minibus is facing west
- the incidence of solar radiation in zone 1 is higher, as the ratio of the glazed surface is greater than in zone 2, and the windshield has an inclination of 45° with respect to the horizontal plane
- the glazing of zone 2 is tinted and consequently has a lower transmissivity.

The model reproduces the experimental temperatures of the internal masses fairly accurately, although with a small overprediction in the case of zone 2. However, whereas

the internal air is mixed and the measured air temperature does not depend much on the thermocouple positioning, the measurements of the temperatures of internal masses are strongly dependent on thermocouple location. For instance, the temperature of the seats depends on the incident radiation on each of them. Consequently, more thermocouples would be necessary to obtain experimentally a precise mean internal masses temperature.

4.3 Estimation of the cooling capacity

The developed model has been applied to estimate the cooling capacity that the vehicle needs to maintain thermal comfort inside the cabin. The 2015 ASHRAE Handbook-HVAC Applications (ASHRAE, 2015) recommends the following conditions for the summer season:

- temperature inside the vehicle cabin between 16 to 27°C
- relative humidity of 50%
- outdoor air intake of 2.5 to 5 l/s per passenger.

The thermal loads included in the model are occupation gains, auxiliary equipment, and ventilation. One person has been considered for zone 1 (driver), and 17 passengers for zone 2 (fully occupied). The main electrical auxiliaries are the blowers of the A/C system, which also cause a heat gain inside the cabin. Their associated heat load is introduced directly into the model from manufacturer data. Thus, a typical minibus has one A/C blower installed in the dashboard and it consumes 290 W at its maximum speed. Two additional blowers are installed at the rear of the vehicle and they consume 247 W each.

The target indoor thermal conditions are 25°C, 50% relative humidity and the outdoor air intake of 5 l/s per passenger.

The external conditions of radiation and ambient temperature used to determine the cooling capacity correspond to the first day of test 3. Figure 12 depicts the balance of the solar heat gains in the vehicle cabin. The total incident solar radiation is either absorbed by the walls or windows, transmitted towards the inside of the vehicle, or blocked (reflected by glazing or external walls).

The solar radiation absorbed by the walls increases their internal energy and consequently their internal surface temperature, which in turn induces a convective heat gain for the internal air. The transmitted radiation goes directly inside the cabin and hits on the internal walls and masses. As the energy emitted from the internal walls is in the form of long wave radiation, it cannot escape freely through the windows. Therefore, the air inside the cabin warms as in the greenhouse effect.

According to Figure 12, during a day (24 h), around 66% of the solar radiation is absorbed and transmitted into the cabin. Approximately 53% of the total incident radiation is absorbed by the minibus surfaces, and 13% is from transmission through the window glazing towards the inside the cabin. In addition, despite the transmissivity of the glazing, around 34% of the incident radiation does not enter the cabin, due to the fact that not all the surfaces are fully covered by glazing, and due to the variable angle of incidence (generally not perpendicular to the glazing); consequently some solar radiation is blocked and reflected out of the vehicle.

Figure 12 Balance of solar heat gains in the minibus cabin (see online version for colours)

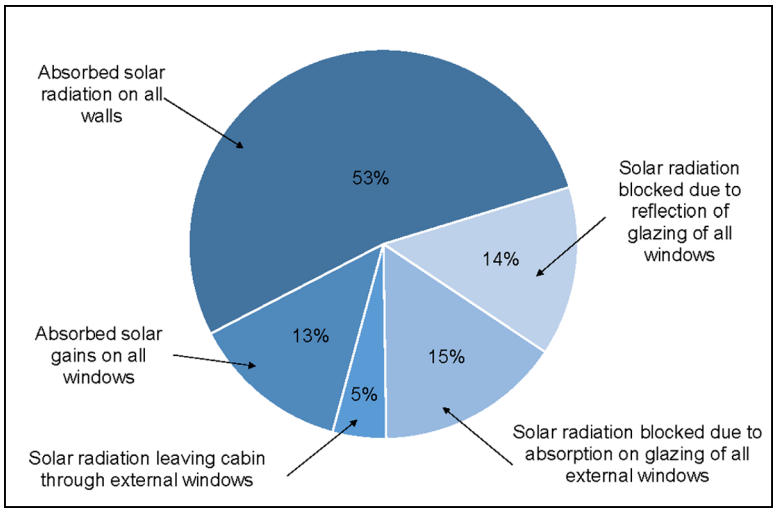

The cooling capacity is determined by the sensible loads ($\dot{Q}_{sen}$) and the latent loads ($\dot{Q}_{lat}$) of the vehicle cabin. The latent loads include ventilation, infiltration, coupling, internal latent gains and vapour adsorption in the walls. The sensible loads consider the infiltration and ventilation gains, the energy transmitted into and stored in the walls, the absorbed solar gains on all inside surfaces of zones (walls and windows) and the internal gains. The internal gains (convective and radiative) are constant since they depend on the number of passengers and on the auxiliary equipment. These energy loads are obtained from two outputs of Types 56, NTYPE 31 and NTYPE 11 (TRNSYS v. 16.1, 2007).

Figure 13 Cooling capacity of the minibus cabin (see online version for colours)

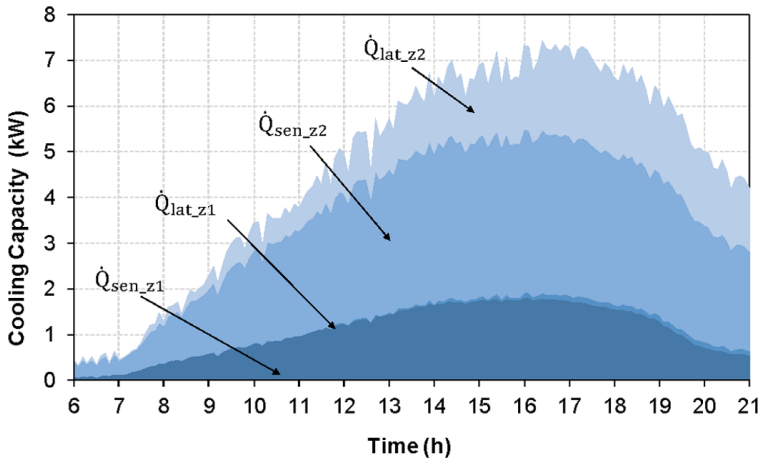

Figure 13 shows the cooling capacity calculated over 15 h for each zone. The variation of the cooling capacity corresponds to the variation in the incident solar radiation on the

vehicle cabin. The main loads that influence the sensible load are the solar and the internal gains. The solar gain varies according to the outdoor conditions (solar radiation and outdoor temperature). The maximum cooling capacity is obtained around three hours after the maximum incident solar radiation, at approximately the same time as the maximum outdoor temperature. According to Figure 13, the maximum cooling capacity is 7.4 kW, which is reached with $T_{amb} = 29.1°C$ and $I = 945.8$ W/m^2. The percentage of the sensible load is 72%, with 28% as a latent load.

Zone 2 needs more air flow and ventilation. In the same direction, the sensible heat demand $\dot{Q}_{sen}$ in zone 2 is higher for the following reasons: the load due to the solar radiation through the glazings; the load transmission and radiation through the external surfaces; the load transmitted by the outside air infiltration; and the load due to internal contributions such as the passengers and the auxiliary equipment (blowers).

5 Conclusions and future work

In this paper, a dynamic thermal model of a minibus cabin has been developed in TRNSYS considering the different materials and geometrical features of the vehicle. The model is able to predict the cabin's thermal behaviour under transient conditions (ambient temperature and solar radiation). Two thermal zones were considered in the model due to the different incidence of the sun on each side of the vehicle, which consequently affects the local thermal comfort in each zone.

Using TRNSYS has the advantage of an already reliable model for the calculation of thermal loads (Type 56) for real outdoor conditions. The main drawback, which is not related to the software tool itself, is that this approach requires the fitting of parameters such as the air exchange rate between zones, and consequently experimental tests have to be carried out in order to aquire a reliable simulation tool.

The model validation was conducted with the minibus parked inside and outside a garage under variable ambient conditions. The model accurately reproduces the warm-up and cool-down of the vehicle cabin.

A solar gain analysis was performed using the proposed model. The results show that approximately 53% of the total incident radiation is absorbed by the minibus surfaces, 13% is transmitted by the windows glazing to the inside of the cabin, and the remaining 34% is blocked and reflected towards outside of the vehicle.

In addition, the developed model has been employed to determine the cooling capacity required to maintain thermal comfort inside the cabin. The study was conducted during a day (24 h), and for a minibus that was considered to be fully occupied. The maximum cooling capacity was 7.4 kW of which 72% was due to the sensible load and 28% due to the latent load.

The current model can predict the load in real outdoor conditions with no particular shadows on the vehicle (e.g., extra urban conditions). In future work, a model will be developed to calculate the thermal loads in urban driving cycles. Such a model has to include traffic information to know where the vehicle is at each point in time, and a geometric model of the surrounding buildings, in order to calculate the shadows which are created by them.

Acknowledgements

Daniela C. Vásconez-Núñez acknowledges the financial support provided by the CONVOCATORIA ABIERTA 2013-SEGUNDA FASE program, which was funded by the SENESCYT (Secretaría Nacional de Educación Superior, Ciencia, Tecnología e Innovación) (Grant No 2014-AR3R7463) of Ecuador.

References

Akyol, M. and Kilic, M. (2010) 'Dynamic simulation of HVAC system thermal loads in an automobile compartment design', *International Journal of Vehicle*, Vol. 52, pp.177–198.

ASHRAE (2014) *ASHRAE Handbook REFRIGERATION*, ASHRAE, Atlanta, pp.24.3–24.5.

ASHRAE (2015) *ASHRAE Handbook Heating, Ventilating and Air-Conditioning Applications*, ASHRAE, Atlanta, pp.11.1–11.3.

Conceição, E., Silva, M., André, J. and Viegas, D.X. (1999) *A Computational Model to Simulate the Thermal Behaviour of the Passengers Compartment of Vehicles*, SAE Technical Paper, Volume 01-0778.

Dullinger, C., Struckl, W. and Kozek, M. (2015) 'A modular thermal simulation tool for computing energy consumption of HVAC units in rail vehicles', *Applied Thermal Engineering*, Vol. 78, pp.616–629.

Fayazbakhsh, A.M. and Bahrami, M. (2013) *Comprehensive Modeling of Vehicle Air Conditioning Loads Using Heat Balance Method*, SAE Thecnical Paper.

Gosney, W.B. and Olama, H.A.L. (1975) 'Heat and enthalpy gains through cold rooms doorways', *Proceedings of the Institute of Refrigeration*, Vol. 72, pp.31–41.

Incropera, F.P., De Witt, D.P., Bergman, T.L. and Lavine, A.S. (2007) *Fundamentals of Heat and Mass Transfer*, Jonh Wiley & Sons, USA.

International Organization of Motor Vehicle Manufacturers (n.d.) *OICA*, [Online] Available at: http://www.oica.net/ (Accessed 9 February, 2016).

Knibbs, L.D., de Deara, R.J. and Atkinson, S.E. (2009) 'Field study of air change and flow rate in six automobiles', *International Journal of Indoor Environment and Health*, Vol. 19, pp.303–3013.

Lee, H., Hwang, Y., Song, I. and Jang, K. (2015) 'Transient thermal model of passenger car's cabin and implementation to saturation cycle with alternative working fluids', *Energy*, Vol. 90, pp.1859–1868.

Levinson, R., Pan, H., Ban-Weiss, G., Rosado, P., Paolini, R. and Akbari, H. (2011) 'Potenctial benefits of solar reflective car shells: cooler cabins, fuel savings and emission reductions', *Applied Energy*, Vol. 88, pp.4343–4357.

Marcos, D., Francisco, J.P., Bordons, C. and Guerra, J. (2014) 'The development and validation of a thermal model for the cabin of a vehicle', *Applied Thermal Engineering*, Vol. 66, pp.646–656.

Mezrhab, A. and Bouzidi, M. (2006) 'Computation of thermal comfort inside a passenger car compartment', *Applied Thermal Engineering*, Vol. 26, pp.1697–1704.

Ott, W., Klepeis, N. and Switzer, P. (2008) 'Air change rates of motor vehicles and in-vehicle pollutant concentrations', *Journal of Exposure Science and Environmental Epidemiology*, Vol. 18, pp.312–325.

Pokorny, J., Fiser, J. and Jicha, M. (2014) 'Virtual testing stand for evaluation of car cabin indoor enviroment', *Advances in Engineering Software*, Vol. 76, pp.48–55.

Roy, D., Petitjean, P. and Clodic, D. (2003) *Influence of Various Heat Transfers on Passenger Thermal Comfort*, SAE Technical Paper.

Sevilgen, G. and Kilic, M. (2010) 'Transient numerical analysis of airflow and heat trnsfer in a vehicle cabin during heating period', *International Journal of Vehicle Design*, Vol. 52, pp.144–158.

Shimizu, S., Hara, H. and Asakawa, F. (1984) 'Analysis on Air-Conditioning heat load of a passenger vehicle', *International Journal of Vehicle Desing*, Vol. 4, pp.292–311.

Torregrosa-Jaime, B., Bjurling, F., Corberán, J.M. and Di Sciullo, F. (2015) 'Transient thermal model of a vehicle´s cabin validated under variable ambient conditions', *Applied Thermal Engineering*, Vol. 75, pp.45–53.

TRNSYS 16 Documentation (2007) *Multizone Building modeling with Type56 and TRNBuild*, Solar Energy Laboratory, University of Wisconsin-Madison, pp.116–169.

TRNSYS v. 16.1 (2007) *A Transient System Simulation Program*, Solar Energy Laboratory, University of Wisconsin.

Nomenclature

α_{Ra_L}	Thermal diffusivity [$m^2\ s^{-1}$]
κ	Thermal conductivity [$W\ m^{-1}\ K^{-1}$]
β	Volumetric thermal expansion coefficient [K^{-1}]
ρ	Density [$kg\ m^{-3}$]
ν	Kinematic viscosity [$m^2\ s^{-1}$]
A	Area [m^2]
A/C	Air conditioning
CFD	Computational fluid dynamics
FH	Fan heaters
F_m	Density factor
g	Acceleration of gravity [$m\ s^{-2}$]
H	Height [m]
$\overline{h}$	Convective coefficient [$W\ m^{-2}\ K^{-1}$]
HVAC	Heating, ventilating and air conditioning
$\overline{\mathrm{Nu}}_L$	Number of Nusselt
L	Length [m]
$\dot{Q}$	Heat load [W]
Pr	Prandtl number
Ra_L	Rayleigh
T	Temperature [°C]
z	Zone
Subscripts	
amb	Ambient
f	Film

lat	Latent energy
sen	Sensible
surf	Surface
1	Zone 1
2	Zone 2